Langmuir
Article
pubs.acs.org/Langmuir

Synthesis of Silver Nanoparticles Coated with OH-Functionalized Organic Groups: Dispersion and Covalent Bonding in Epoxy Networks

Ignacio E. dell'Erba, Cristina E. Hoppe,* and Roberto J. J. Williams

Institute of Materials Science and Technology (INTEMA), University of Mar del Plata and National Research Council (CONICET), J. B. Justo 4302, 7600 Mar del Plata, Argentina

Received July 14, 2009. Revised Manuscript Received August 27, 2009

The introduction of reactive functionalities in the organic groups used to stabilize inorganic nanoparticles (NPs) enables multiple applications based on their covalent fixation to a variety of materials, substrates and interfaces. In this paper we report the synthesis of silver nanoparticles (NPs) with an average diameter of about 4 nm, coated with particular organic groups that allow their solubility in a variety of organic solvents and the covalent bonding through secondary hydroxyl groups present in their structure. Water-dispersible NPs stabilized with 11-mercaptoundecanoate anions were first synthesized. The esterification of carboxylate groups with phenyl glycidyl ether generated 2-hydroxy-ester functionalities and made the NPs dispersible in a variety of organic solvents. To illustrate the multiple possible applications of the synthesized NPs, their incorporation to an epoxy network is discussed. A solution of the silver NPs in diglycidyl ether of bisphenol A was polymerized in the presence of benzyldimethylamine as initiator. This led to an epoxy network containing a homogeneous dispersion of silver NPs as revealed by the constancy of the plasmon band location. Covalent bonding of the NPs to the epoxy matrix was produced by chain transfer reactions involving the hydroxyl groups. Nanocomposites were strongly colored and exhibited a dependence of the glass transition temperature on the concentration of NPs. Several applications are envisaged for these materials.

Introduction

Combination of polymers with inorganic nanoparticles (NPs) offers enormous possibilities for the design of functional materials with important technological applications. Dispersion of metal NPs in polymeric matrices can be applied for the development of embedded capacitors,[1] ultralow refractive index materials,[2] sensors,[3] surface enhanced Raman spectroscopy (SERS) substrates,[4] holographic composites,[5] antibacterial fibers,[6] etc. Macroscopic performance of these materials strongly depends on the possibility to tune the spatial distribution of the NPs in the matrix avoiding uncontrolled aggregation phenomena that would preclude any advantages associated with the use of particles of nanoscopic dimensions.[7] Typical approaches used to minimize aggregation include proper functionalization of the nanoparticles to make them compatible with the polymeric host[7,8] and selection of an adequate process to diminish the probability of clustering (e.g., rapid precipitation, mechanical blending, ultrasonication, etc.).[8,9] For many applications, control on the geometrical distribution of the NPs in the matrix is also necessary, which requires the use of external fields,[10] templates[7,10] or careful selection of the polymer matrix/NPs functionalization combination.[11]

Nanostructured epoxy networks are a relatively new class of advanced materials that exhibit enhanced properties (i.e., toughness, modulus, strength, permeability, surface energy) with respect to those of the matrix or add new functional properties (i.e., electrical, optical, magnetic). Nanostructured epoxies are usually obtained by adding amphiphilic block copolymers to epoxy formulations,[12−15] or by dispersing different types of NPs such as silica nanoparticles,[16] polyhedral oligomeric silsesquioxanes (POSS),[17−20] nanoclays,[21−24] or carbon nanotubes (CNT).[25−28] However, the use of epoxies and other cross-linked polymer

*To whom correspondence should be addressed. E-mail: hoppe@fi.mdp.edu.ar.

(1) Qi, L.; Lee, B. I.; Chen, S.; Samuels, W. D.; Exarhos, G. J. *Adv. Mater.* **2005**, *17*, 1777.
(2) Althues, H.; Henle, J.; Kaskel, S. *Chem. Soc. Rev.* **2007**, *36*, 1454.
(3) Luechinger, N.; Loher, S.; Athanassiou, E. K.; Grass, R. N.; Stark, W. J. *Langmuir* **2007**, *23*, 3473.
(4) Hasell, T.; Lagonigro, L.; Peacock, A. C.; Yoda, S.; Brown, P. D.; Sazio, P. J. A.; Howdle, S. M. *Adv. Funct. Mater.* **2008**, *18*, 1265.
(5) Goldenberg, L. M.; Sakhno, O. V.; Smirnova, T. N.; Helliwell, P.; Chechik, V.; Stumpe, J. *Chem. Mater.* **2008**, *20*, 4619.
(6) Kong, H.; Jang, J. *Langmuir* **2008**, *24*, 2051.
(7) Balazs, A. C.; Emrick, T.; Russell, T. P. *Science* **2006**, *314*, 1107.
(8) Krishnamoorti, R. *MRS Bull.* **2007**, *32*, 341.
(9) Mackay, M. E.; Tuteja, A.; Duxbury, P. M.; Hawker, C. J.; Van Horn, B.; Guan, Z.; Chen, G; Krishnan, R. S. *Science* **2006**, *311*, 1740.
(10) Vaia, R. A.; Maguire, J. F. *Chem. Mater.* **2007**, *19*, 2736.
(11) Akcora, P.; Liu, H.; Kumar, S. K.; Moll, J.; Li, Y.; Benicewicz, B. C.; Schadler, L. S.; Acehan, D.; Panagiotopoulos, A. Z.; Pryamitsyn, V.; Ganesan, V.; Ilavsky, J.; Thiyagarajan, P.; Colby, R. H.; Douglas, J. F. *Nat. Mater.* **2009**, *8*, 354.
(12) Hillmyer, M. A.; Lipic, P. M.; Hajduk, D. A.; Almdal, K.; Bates, F. S. *J. Am. Chem. Soc.* **1997**, *119*, 2749.
(13) Dean, J. M.; Verghese, N. E.; Pham, H. Q.; Bates, F. S. *Macromolecules* **2003**, *36*, 9267.
(14) Ritzenthaler, S.; Court, F.; Girard-Reydet, E.; Leibler, L.; Pascault, J. P. *Macromolecules* **2003**, *36*, 118.
(15) Meng, F.; Zheng, S.; Zhang, W.; Li, H.; Liang, Q. *Macromolecules* **2006**, *39*, 711.
(16) Hartwig, A.; Sebald, M.; Kleemeier, M. *Polymer* **2005**, *46*, 2029.
(17) Crivello, J. V.; Malik, R. *J. Polym. Sci., Part A: Polym. Chem.* **1997**, *35*, 407.
(18) Matějka, L.; Strachota, A.; Pleštil, J.; Whelan, P.; Steinhart, M.; Šlouf, M. *Macromolecules* **2004**, *37*, 9449.
(19) Liu, H.; Zheng, S.; Nie, K. *Macromolecules* **2005**, *38*, 5088.
(20) Zucchi, I. A.; Galante, M. J.; Williams, R. J. J.; Franchini, E.; Galy, J.; Gerard, J. F. *Macromolecules* **2007**, *40*, 1274.
(21) Park, J. H.; Jana, S. C. *Macromolecules* **2003**, *36*, 2758.
(22) Le Pluart, L.; Duchet, J.; Sautereau, H.; Gerard, J. F. *Macromol. Symp.* **2003**, *194*, 155.
(23) Ogasawara, T.; Ishida, Y.; Ishikawa, T.; Aoki, T.; Ogura, T. *Composites, Part A* **2006**, *37*, 2236.
(24) Boukerrou, A.; Duchet, J.; Fellahi, S.; Kaci, M.; Sautereau, H. *J. Appl. Polym. Sci.* **2007**, *103*, 3547.
(25) Liu, J.; Rinzler, A. G.; Dai, H.; Hafner, J. H.; Bradley, R. K.; Boul, P. J.; Lu, A.; Iverson, T.; Shelimov, K.; Huffman, C. B.; Rodriguez-Macias, F.; Shon, Y. S.; Lee, T. R.; Colbert, D. T.; Smalley, R. E. *Science* **1998**, *280*, 1253.
(26) Wang, Q.; Dai, J.; Li, W.; Wei, Z.; Jiang, J. *Compos. Sci. Technol.* **2008**, *68*, 1644.
(27) Warren, G. L.; Sun, L.; Hadjiev, V. G.; Davis, D.; Lagoudas, D.; Sue, H. J. *J. Appl. Polym. Sci.* **2009**, *112*, 290.
(28) Auad, M. L.; Mosiewicki, M. A.; Uzunpinar, C.; Williams, R. J. J. *Compos. Sci. Technol.* **2009**, *69*, 1088.

matrices as hosts for the dispersion of metal NPs has been scarcely reported in spite of their potentiality for the design of high performance nanocomposites. Common procedures to obtain these materials involve adequate coating of NPs to optimize the formation of an initially well-dispersed reactive system.[29−31] However, polymerization can induce the phase separation of a NPs-rich phase[32] producing domains trapped in the generated polymer.[33,34] An interesting way to overcome this problem consists in considering NPs as coreactants or comonomers susceptible to be incorporated in the polymer structure during the polymerization reaction. This approach not only minimizes the probability of clustering and surface segregation but also fixes the NPs to the polymer avoiding migration phenomena. This is particularly important for applications in which the material is in contact with solvents or subject to temperatures that could increase NPs diffusion rate. Some examples of covalent attachment of NPs to cross-linked polymeric hosts can be found in the reinforcing of epoxy matrices with silica NPs,[16] in the cross-linking of amine-terminated P(VDF-*co*-CTFE) with carboxylic acid-covered TiO_2 nanoparticles[35] and in the synthesis of magnetoresponsive gels involving iron nanoparticles as functional cross-linkers by surface-initiated ATRP.[36]

In this study we report the synthesis of silver NPs stabilized with organic groups bearing secondary hydroxyls as reactive functionalities and their dispersion and covalent bonding into an epoxy network. In a first step water-dispersible silver NPs stabilized by 11-mercaptoundecanoate anions were synthesized. In a second step carboxylate groups were esterified with phenyl glycidyl ether generating 2-hydroxyester functionalities. The presence of OH groups enables the covalent bonding of the silver NPs to a variety of materials, substrates and interfaces. The dispersion and covalent bonding of the functionalized silver NPs into an epoxy network was produced by chain transfer reactions in the course of the homopolymerization of an epoxy monomer initiated by a tertiary amine.[37] Final properties of the resulting nanocomposites (UV−visible absorption, glass transition temperatures and extent of NPs attachment to the network) are evaluated and discussed for different concentrations of NPs in the epoxy matrix.

Experimental Section

Synthesis of 11-Mercaptoundecanoic Acid-Coated Silver NPs (Ag@MUA). Ag@MUA NPs were synthesized by direct reduction of silver nitrate (Cicarelli, P.A.) in the presence of 11-mercaptoundecanoic acid (MUA, 95 wt % Aldrich). A 20 mL solution of MUA (450 mg, 2 mmol) in THF was added onto 120 mL of a THF/H_2O (volume ratio 5:1) silver nitrate solution containing 170 mg of $AgNO_3$ (1 mmol) under vigorous stirring. The initially transparent solution became yellow and turbid by formation of silver thiolate.[38] After 5 min, 10 mL of a freshly prepared 1 M $NaBH_4$ (Fluka ≥96 wt %) aqueous solution was rapidly added provoking the formation of a black solid that immediately precipitated to the bottom of the flask. After separation of the supernatant by decantation, the solid was purified three times by successive dispersion/precipitation cycles with water/THF to eliminate most of the unattached MUA. The purified solid was dispersed in 20 mL of distilled water and annealed by refluxing at $T \approx 140$ °C for 24 h to increase the average size and narrow the size distribution of the NPs. After this process, NPs dispersion was centrifuged at 12 000 rpm to eliminate any insoluble solids and purified through precipitation/dispersion cycles with hot ethanol and THF. The final product was dispersed in 20 mL of distilled water.

Esterification of Ag@MUA NPs with Phenyl Glycidyl Ether (PGE). For esterification of carboxylate groups of Ag@MUA NPs with PGE, 10 mL of the aqueous dispersion of NPs was mixed with 266 μL (2 mmol) of PGE (Aldrich, 99 wt %) and 27.0 mg (0.1 mmol) of triphenylphosphine (TPP, Fluka, purum). The reaction was carried out at 90 °C in a two-phase dispersion under vigorous stirring. After two hours, the solid formed was separated by decantation and dispersed in chloroform. NPs were precipitated using absolute ethanol and separated by centrifugation at 10 000 rpm for 10 min. The solid was dispersed in 3 mL of chloroform and stored for subsequent use. Concentration estimated by gravimetric analysis was 6.6 mg of coated NPs/mL.

Synthesis of Epoxy Nanocomposites. The diepoxy monomer was based on diglycidyl ether of bisphenol A (DGEBA, DER 332, Dow), with a mass per mole of epoxy groups equal to 174.3 g/mol. The tertiary amine used as initiator of the anionic polymerization was benzyldimethylamine (BDMA, Sigma). Selected volumes of esterified NPs dispersed in chloroform were blended with DGEBA. After chloroform evaporation, an amount of 0.06 mol of BDMA per mol of epoxy groups was added with continuous stirring at room temperature. The resulting solutions were strongly colored but optically homogeneous. Samples of about 200 μm thickness were obtained in a mold consisting of two glass plates spaced by two strips of adhesive tape and held together with clamps. To obtain monoliths, the solution was cast into polypropylene (PP) molds (Eppendorf vials). Samples were placed in an oven and polymerized for 3 h at 100 °C. The neat epoxy network was obtained following a similar schedule.

Techniques. The size distribution of silver NPs was determined using a Philips CM-12 transmission electron microscope (TEM) operated at an accelerating voltage of 100 kV. Samples were prepared by dropping 6 μL of a dispersion of the particles on a copper grid coated with Formvar and a carbon film.

The organic/inorganic percentages in the synthesized NPs (before and after esterification) were determined by thermogravimetry (Shimadzu TGA-50H). Dynamic scans were performed under nitrogen flow at 20 °C/min between 30 and 1000 °C.

The plasmon band of the solution of NPs was recorded with an Agilent 8453 diode array spectrophotometer. Samples were placed in a 1 cm × 1 cm × 3 cm quartz cell and spectra recorded at room temperature. The same device was used to determine the spectra of the 200 μm thickness nanocomposites. A special cell for solid samples was used for this purpose.

Middle-infrared spectroscopy (MIR, Genesis II, Mattson) was employed to characterize NPs before and after esterification. Measurements were carried out using KBr disks impregnated with drops of the NPs dispersions. The glass transition temperature (T_g) was determined by differential scanning calorimetry (DSC, Perkin-Elmer Pyris 1), from midpoint values of the change in specific heat in heating scans performed at 10 °C/min (two runs were performed for every composition).

Leaching tests were performed by immersion of a slice of each nanocomposite sample in THF at room temperature during three months and subsequent analysis of the supernatants by UV−vis spectrophotometry.

(29) Pardiñas-Blanco, I.; Hoppe, C. E.; López-Quintela, M. A.; Rivas, J. *J. Non-Cryst. Solids* **2007**, *353*, 826.
(30) Pérez-Juste, J.; Correa-Duarte, M. A.; Liz-Marzán, L. M. *Appl. Surf. Sci.* **2004**, *226*, 137.
(31) Boev, V. I.; Pérez-Juste, J.; Pastoriza-Santos, I.; Silva, C. J. R.; Gomes, M. J. M.; Liz-Marzán, L. M. *Langmuir* **2004**, *20*, 10268.
(32) Soulé, E. R.; Borrajo, J.; Williams, R. J. J. *Macromolecules* **2007**, *40*, 8082.
(33) Zucchi, I. A.; Hoppe, C. E.; Galante, M. J.; Williams, R. J. J.; López-Quintela, M. A.; Matějka, L.; Slouf, M.; Pleštil, J. *Macromolecules* **2008**, *41*, 4895.
(34) Gómez, M. L.; Hoppe, C. E.; Zucchi, I. A.; Williams, R. J. J.; Giannotti, M. I.; López-Quintela, M. A. *Langmuir* **2009**, *25*, 1210.
(35) DiMaio, J. R.; Kokuoz, B.; Ballato, J. *J. Am. Chem. Soc.* **2008**, *130*, 5628.
(36) Czaun, M.; Hevesi, L.; Takafuji, M.; Ihara, H. *Chem. Commun.* **2008**, 2124.
(37) Pellice, S. A.; Fasce, D. P.; Williams, R. J. J. *J. Polym. Sci., B: Polym. Phys.* **2003**, *41*, 1451.
(38) Parikh, A. N.; Gillmor, S. D.; Beers, J. D.; Beardmore, K. M.; Cutts, R. W.; Swanson, B. I. *J. Phys. Chem. B* **1999**, *103*, 2850.

Results and Discussion

Synthesis of Ag@MUA NPs. A large variety of experimental techniques has been developed in recent years to synthesize metal NPs coated with different stabilizing thiols. Metal protected clusters (MPCs) coated with alkanethiols can be obtained and subsequently modified in their functionalization through the well-known "place exchange reaction" developed by Murray's group.[39] Kinetic results obtained for gold NPs show that the rate of ligand exchange depends on several factors like concentration, size of the entering ligand and chain length of the protecting monolayer. As an example of the use of this procedure to incorporate thiocarboxylic acids, Simard et al.[40] developed amphiphilic gold NPs through place exchange of octanethiol with MUA.

An alternative procedure to join a thiocarboxylic acid to the surface of a metal particle is the direct reduction of a metallic precursor in its presence. To our knowledge, the first one-step successful preparation of thiocarboxylic acid-coated water dispersible metal NPs was reported by Kimura's group, who developed a simple and high yield method for the synthesis of mercaptosuccinic acid (MSA)-coated gold and silver NPs.[41] They demonstrated that a metal precursor solution in an organic solvent can be reduced in the presence of a thiocarboxylic acid to give a powder constituted by carboxylate-functionalized metal NPs. The thiol group is joined to the surface of the metal, whereas the acid group functionality is exposed to the environment. This makes NPs very polar, susceptible to reactive functionalization and easily dispersible in water. Main results reported by this group correspond to the synthesis of gold colloids which could be used to form colloidal crystals with a high level of order.[42] Polydispersity of silver NPs obtained by this method is usually higher than in the case of gold,[43] although highly ordered superlattices could still be obtained by previous fractionation or by self-correction during the assembly process.[44] Using this general method as a starting point we developed a modified synthesis process to obtain MUA-coated silver NPs dispersible in water. Our aim was to obtain very small silver NPs or clusters that could be subsequently thermally annealed to increase the average size of NPs and narrow the size distribution. The use of an annealing process was reported by Maye et al.[45] to obtain alkylthiol-coated gold NPs of narrower size distribution and bigger size starting from 2 nm gold colloids obtained by the Brust−Schiffrin method.[46]

To obtain very small silver NPs in the first step of the synthesis we used an excess of MUA to retard core growth and an environment favoring fast insolubilization of the NPs generated.[47] A THF solution of MUA was mixed with a silver nitrate solution in THF/H_2O to form a fine and slightly turbid dispersion of the yellow silver thiolate.[38] Subsequently, an aqueous solution of the reducing agent ($NaBH_4$) was rapidly added to this dispersion. The use of THF/H_2O (5:1) as solvent provides the right environment to allow the initial solubilization of silver nitrate and the fast precipitation of MUA-coated NPs after reduction. Hydrolysis of $NaBH_4$ raised the pH value of the initially acid solution to almost 10, inducing ionization of the acid groups and producing the fast precipitation of the sodium salt of the MUA-coated silver NPs. This solid was separated from the supernatant and easily redispersed in pure distilled water to give a dark-red stable colloidal solution.

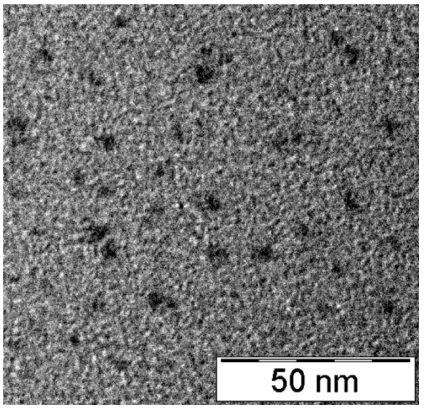

Figure 1. TEM image of MUA-coated silver NPs after the first step of the synthesis.

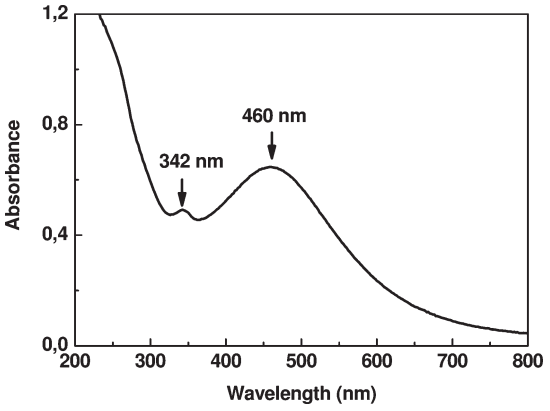

Figure 2. UV−visible spectrum of MUA-coated silver NPs after the first step of the synthesis.

Figure 1 shows a typical TEM image of the Ag@MUA NPs produced after the first step of the synthesis, in which low-contrast aggregates, apparently formed by tiny clusters, are observed. An UV−visible spectrum of these silver NPs can be observed in Figure 2. A broad band centered at 460 nm is clearly shown, along with a smaller peak at 342 nm. These peak values are different from commonly reported plasmon band positions of small silver NPs, normally found between 400 and 435 nm, depending on coating and solvent.[43,48]

A red shift of the plasmon band has been reported for particles generated in the first stages of some synthetic procedures,[48] and for water-dispersible clusters of few atoms.[49] Harb et al.[50] reported experimental results and theoretical calculations for Ag_n clusters (4−22 atoms) embedded in an argon matrix. They showed that for small n values spectra are characterized by a strong optical response in the 3.0−5.0 eV range (414−248 nm range) with several narrow or broad peaks, while for $n \geq 12$ they

(39) Templeton, A. C.; Wuelfing, W. P.; Murray, R. W. *Acc. Chem. Res.* **2000**, *33*, 27 and references therein.
(40) Simard, J.; Briggs, C.; Boal, A. K.; Rotello, V. M. *Chem. Commun.* **2000**, 1943.
(41) Chen, S.; Kimura, K. *Langmuir* **1999**, *15*, 1075.
(42) Wang, S.; Sato, S.; Kimura, K. *Chem. Mater.* **2003**, *15*, 2445.
(43) Chen, S.; Kimura, K. *Chem. Lett.* **1999**, 1169.
(44) Yang, Y.; Kimura, K. *J. Phys. Chem. B* **2006**, *110*, 24442.
(45) Maye, M. M.; Zheng, W.; Leibowitz, F. L.; Ly, N. K.; Zhong, C. *Langmuir* **2000**, *16*, 490.
(46) Brust, M.; Walker, M.; Bethell, D.; Schiffrin, D. J.; Whyman, R. *Chem. Commun.* **1994**, 801.
(47) Abad, J. M.; Sendroiu, I. E.; Gass, M.; Bleloch, A.; Mills, A. J.; Schiffrin, D. J. *J. Am. Chem. Soc.* **2007**, *129*, 12932.
(48) He, S.; Yao, J.; Jiang, P.; Shi, D.; Zhang, H.; Xie, S.; Pang, S.; Gao, H. *Langmuir* **2001**, *17*, 1571.
(49) Shang, L.; Dong, S. *Chem. Commun.* **2008**, 1088.
(50) Harb, M.; Rabilloud, F.; Simon, D.; Rydlo, A.; Lecoultre, S.; Conus, F.; Rodrigues, V.; Félix, C. *J. Chem. Phys.* **2008**, *129*, 194108.

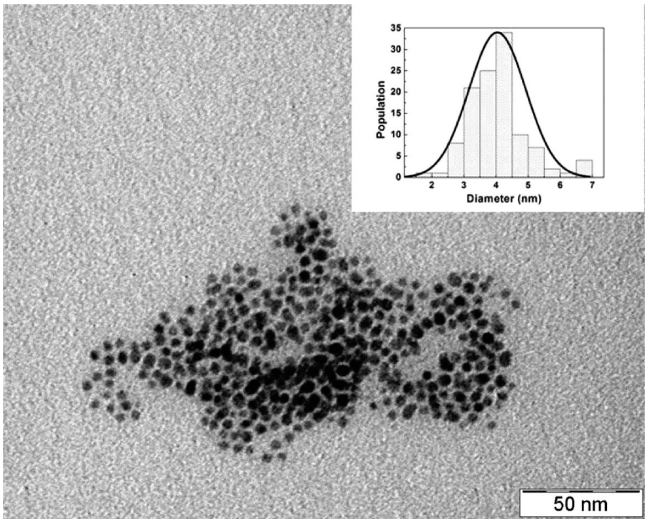

Figure 3. TEM image of MUA-coated silver NPs after the annealing step.

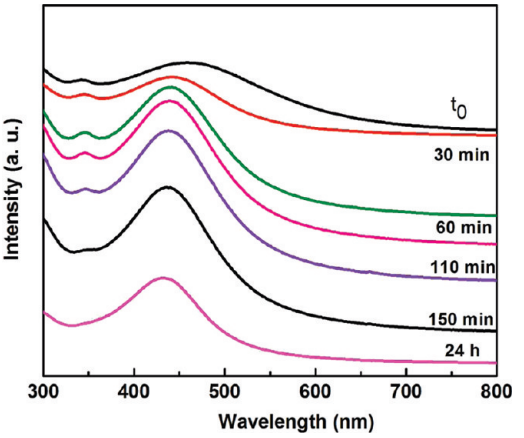

Figure 4. Evolution of UV−visible spectra of MUA-coated silver NPs during the annealing step.

are characterized by a relatively broad band between 3.2 and 3.8 eV (387−326 nm). These results show that the initial spectrum obtained in our synthesis could be consistent with the presence of a distribution of small silver clusters containing few atoms in their structures. Mass and fluorescence characterization of these clusters is a topic of a future work.

The annealing of the silver NPs was carried out by refluxing the water dispersion at $T \approx 140$ °C for 24 h. The initially dark-red dispersion became brown, and a small amount of a precipitate was formed that was separated by centrifugation (although the nature of this small amount of precipitate was not investigated, it may be assumed that the increase in the average size of the NPs is accompanied by the desorption of organic ligands as disulfide salts that do not remain in solution). The remaining solution was purified by repeated precipitation/dispersion cycles, as described in the Experimental Section, to obtain the final distribution of water-dispersible silver NPs.

Figure 3 shows a TEM image of the annealed sample. The average diameter of the NPs increased to 4.0 nm ± 0.9 nm, and the population of small particles (clusters) practically disappeared.

The evolution of UV−visible spectra of MUA-coated silver NPs during the annealing step is shown in Figure 4. The absorption band experienced a blue shift and became narrower with the increase in the annealing time. Moreover, the peak centered at 342 nm, assigned to silver clusters, gradually disappeared during the annealing process. This confirms that the small clusters experienced a coalescence process producing bigger silver NPs with a narrower size distribution. At the end of the annealing process the plasmon band was centered at 432 nm. This value is typical of thiol-capped silver NPs of similar size.[48]

FTIR spectra showed the presence of peaks at 1560 cm^{-1} and 1420 cm^{-1} that can be assigned to the asymmetric and symmetric stretching vibration of carboxylate anions, respectively.[43,51] The counterion was Na^+ as expected from the synthesis and confirmed by XPS spectra. The S−H vibration peak present at 2554 cm^{-1} in pure MUA did not appear in the FTIR spectrum confirming that MUA binds to the silver NPs through the sulfur atoms.

Esterification of Ag@MUA NPs with PGE. Some previous reports on the esterification of carboxylate-modified metal NPs can be found in the literature. Tominaga et al.[51] esterified mercaptosuccinic acid (MSA)-coated Ag NPs with butanol in presence of concentrated sulfuric acid; Shon et al.[52] prepared nanoparticle-core dendrimers by reaction of OH-functionalized dendrons with MUA-coated gold NPs. The approach used in this study to produce the esterification is based on the reaction of carboxylate anions with epoxy groups to produce 2-hydroxyester functional groups (Scheme 1a).

Scheme 1. (a) Reaction of a Carboxylate Anion with an Epoxy Group Leading to a 2-Hydroxyester Functional Group and (b) Chemical Structure of the Organic Ligands after the Esterification Reaction

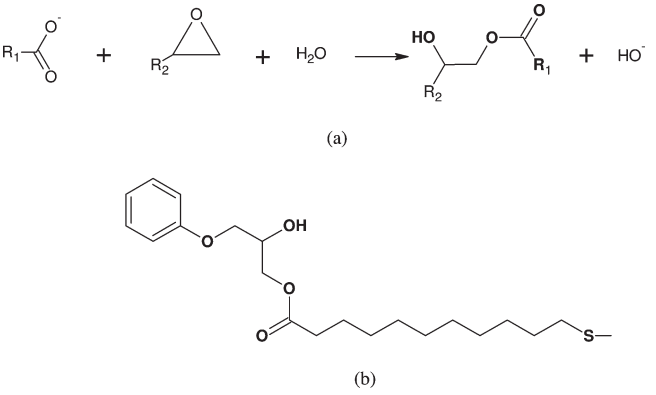

The selected approach has the following advantages: (a) it has no equilibrium limitations enabling to reach conversions close to 100%, (b) it produces a secondary hydroxyl in the structure enabling the functionalization of the organic ligand, (c) the solubility of the resulting NPs in organic solvents can be tuned by an adequate selection of the chemical structure of the epoxy compound, and (d) the reaction can be carried out starting with carboxylic acid groups instead of carboxylate anions by using adequate catalysts such as triphenylphosphine (TPP). It must be taken into account that due to the reactivity of thiol groups with epoxies it was not possible to obtain the structure shown in Scheme 1b by first reacting MUA with PGE and then synthesizing the silver NPs in the presence of the esterified thiol.

In this study we selected phenyl glycidyl ether (PGE) as the epoxy compound to introduce an aromatic ring in the structure of the organic ligands (Scheme 1b). This enabled the dispersibility of the silver NPs in a variety of organic solvents including typical epoxy monomers based on diglycidyl ether of bisphenol A (DGEBA).

(51) Tominaga, J.; Sato, S.; Yao, H.; Kimura, K. *Chem. Lett.* **2002**, 950.

(52) Shon, Y.; Choi, D.; Dare, J.; Dinh, T. *Langmuir* **2008**, *24*, 6924.

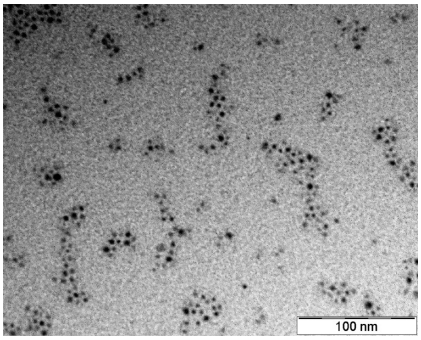

Figure 5. TEM image of the esterified silver NPs.

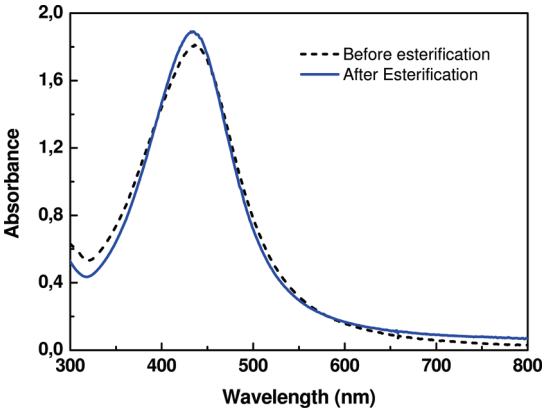

Figure 6. Comparison of plasmon bands of silver NPs before and after esterification.

The esterification was conducted in a two-phase dispersion as described in the Experimental Section. PGE was added in excess with respect to the total amount of MUA added in the first step of the synthesis. TPP was added as a catalyst to allow for the possibility of esterifying carboxylic acid groups if they were formed in the dispersed organic phase. The esterification of carboxylate groups produced the precipitation of the silver NPs. After purification as described in the Experimental Section, the esterified NPs could be dissolved in a variety of organic solvents such as chloroform, acetone, dichloromethane, benzene, etc.

Figure 5 shows a TEM image of the esterified silver NPs. The size distribution was the same as that of the starting NPs, giving direct evidence that coalescence processes did not occur at the conditions selected to produce the esterification. A better proof of the absence of coalescence was obtained by comparing the plasmon bands of the starting silver NPs (dispersed in water) and the esterified NPs (dispersed in chloroform), shown in Figure 6. Both plasmon bands are practically undistinguishable, indicating that NPs kept their original size and solvent effects were negligible.

Apart from the obvious fact of the change in solubility, the occurrence of the esterification reaction and the absence of secondary reactions were confirmed by FTIR spectra. Figure 7 shows an FTIR spectrum of esterified silver NPs in the wavenumber region of interest. The strong carboxylate peaks present at 1560 cm^{-1} and 1420 cm^{-1} in the original material disappeared from the spectra and were replaced by typical ester bands located at 1174 cm^{-1} and 1734 cm^{-1}.[53]

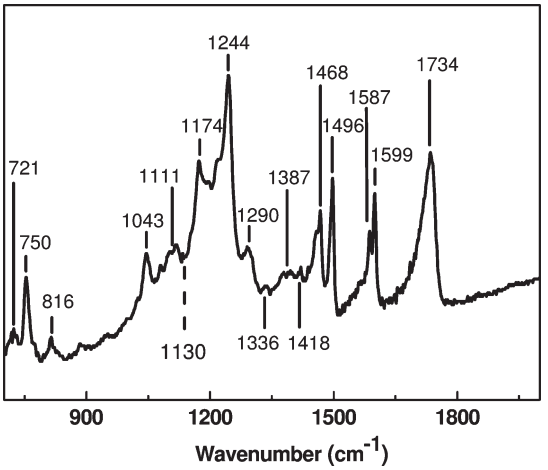

Figure 7. FTIR spectrum of esterified silver NPs.

It might be argued, however, that in the presence of a PGE excess secondary hydroxyls can react with epoxy groups leading to an aliphatic ether and regenerating the secondary hydroxyl. In this way, several PGE units could be attached to the original organic ligand. This possibility was carefully analyzed and finally discarded with the following arguments and experimental evidence:

(a) Alkoxide groups are not stable in water and are rapidly transformed into alcohols; therefore the typical anionic homopolymerization of epoxy groups cannot take place and only the stepwise polyaddition of epoxy to OH groups must be considered. However this reaction is extremely slow and usually insignificant except at high reaction temperatures.[54]

(b) The whole set of peaks present in the FTIR spectrum could be assigned to the structure depicted in Scheme 1b. In the spectral region shown in Figure 7, the following assignment was performed:[53] peaks at 1174 cm^{-1} and 1734 cm^{-1} can be assigned to ester groups, peaks at 750 cm^{-1}, 1468 cm^{-1} (partially), 1496 cm^{-1}, 1587 cm^{-1} and 1599 cm^{-1} are assigned to the aromatic ring, peaks at 1043 cm^{-1} and 1244 cm^{-1} correspond to the aryl ether, peaks at 816 cm^{-1} and 1111 cm^{-1} are characteristic of the secondary alcohol, the peak at 1387 cm^{-1} corresponds to the CH vibration in $O-CH_2$ groups, the peak at 1418 cm^{-1} is assigned to the CH_2 vibration in $CH_2-C=O$ groups, the peak at 1336 cm^{-1} is characteristic of the CH bending in CH−OH groups, and peaks at 721 cm^{-1}, 1290 cm^{-1} and 1468 cm^{-1} (partially) are typical of CH_2 groups. Therefore, every group present in the chemical structure was evidenced by the FTIR spectrum.

(c) The eventual occurrence of a PGE polyaddition to the secondary hydroxyl would lead to an aliphatic ether as the only difference with the structure depicted in Scheme 1b. The aliphatic ether derived from the polyaddition of PGE units exhibits a typical band at 1130 cm^{-1}.[55] This band is absent in the FTIR spectrum shown in Figure 7, confirming that the reaction between the excess PGE and OH groups did not occur at least to a significant extent.

(53) Lin-Vien, D.; Colthup, N. B.; Fateley, W. G.; Graselli, J. G. *The Handbook of Infrared and Raman Characteristic Frequencies of Organic Molecules*; Academic Press: San Diego, 1991.

(54) Riccardi, C. C.; Williams, R. J. J. *J. Appl. Polym. Sci.* **1986**, *32*, 3445.
(55) dell'Erba, I. E.; Williams, R. J. J. *Polym. Eng. Sci.* **2006**, *46*, 351.

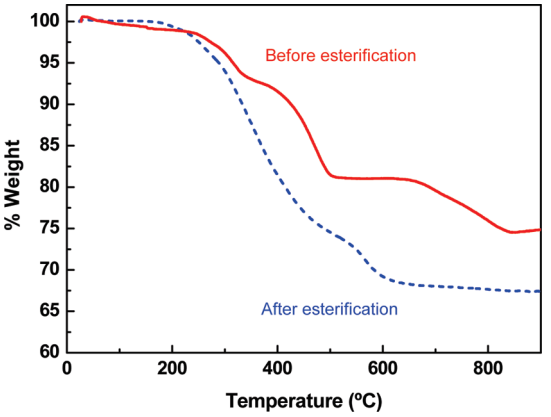

Figure 8. Thermogravimetric curves of silver NPs before and after esterification of the organic ligands with PGE.

(d) The overall mass loss of esterified NPs must be consistent with the assumption that the PGE + OH reaction did not occur. Figure 8 shows the mass loss as a function of temperature for the silver NPs before and after the esterification reaction. The silver NPs stabilized by carboxylate anions (before esterification) exhibit a complex degradation behavior. At low temperatures there is a loss of water adsorbed on the particle surface.[43] Increasing temperature led to consecutive degradation processes that should finally lead to pure silver and sodium-containing products. On the other hand, the esterified silver NPs showed a more simple degradation behavior without any discernible weight loss at low temperatures and a total weight loss of 32.6% at 800 °C. In order to compare this value with the expected mass loss for silver NPs stabilized by organic ligands with the structure shown in Scheme 1b, it is necessary to assume a value of the head area per organic group, $a = (\text{Å}^2)$. For the expected dense packing of alkanethiol chains on metallic NPs this value is close to 21 Å^2.[56] Let us call, d = 40 Å (average diameter of a nanoparticle), $\rho = 1.05 \times 10^{-23}$ g/Å^3 (density of metallic silver), $M = 6.09 \times 10^{-22}$ g/molecule (molar mass of the structure shown in Scheme 1b). The total mass of the nanoparticle is given by the mass of the silver nucleus ($\rho\pi d^3/6$) plus the mass of the attached organic chains ($M\pi d^2/a$). The estimated organic mass fraction is 29.3%, which is consistent with the experimental value. In fact, using an average diameter of NPs of 36 Å instead of 40 Å, that is within the experimental error of the determination, leads to an exact agreement of experimental and estimated mass losses.

Therefore, we can conclude that organic ligands have the structure shown in Scheme 1b and that they present the usual dense grafting to the surface of the silver NPs.

Synthesis and Properties of Epoxy Nanocomposites. Due to the similarity in chemical structures, diglycidyl ether of bisphenol A (DGEBA) was a good solvent for the esterified silver NPs. However, initial solubility does not preclude the existence of a phase separation process in the course of polymerization of the reactive solvent.[32] A convenient way to eliminate this possibility is to produce multiple chemical bonds between the organic ligands stabilizing the NPs and the polymer matrix. In this way, the initial homogeneous dispersion should remain kinetically frozen even in the existence of a thermodynamic driving force to produce phase separation. In our case, the presence of secondary hydroxyl groups in the organic ligands enabled the chemical bonding of NPs to the epoxy network. The tertiary amine used as initiator attacks the epoxy ring producing a quaternary nitrogen cation and an alkoxide anion. The alkoxide initiates the chain homopolymerization of DGEBA by successive reactions with epoxy rings that continuously regenerate an alkoxide group. The OH groups present in the organic ligands act as chain transfer agents. A propagating chain with a terminal alkoxide group terminates by H^+ abstraction from an OH group regenerating an alkoxide group in the organic ligand. In turn, the generated alkoxide initiates a new chain by homopolymerization of epoxy groups enabling the chemical bonding of the NPs to the matrix.

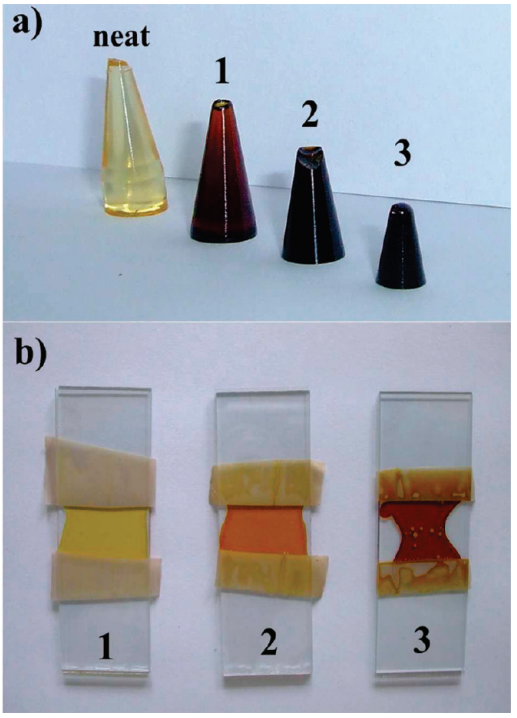

Figure 9. (a) Monoliths and (b) 200 μm thickness films obtained for three different concentrations of coated NPs: 0.06 wt % (nanocomposite 1), 0.19 wt % (nanocomposite 2) and 0.35 wt % (nanocomposite 3). The yellowish monolith is the unmodified epoxy matrix.

Selected volumes of chloroform dispersions of esterified silver NPs were dissolved in diglycidyl ether of bisphenol A (DGEBA). After evaporation of chloroform, strongly colored and homogeneous solutions were obtained. After addition of the initiator (BDMA), solutions containing different concentrations of NPs were polymerized as described in the Experimental Section to obtain the epoxy nanocomposites.

Figure 9 shows monoliths and 200 μm thickness films obtained for three different concentrations of coated NPs: 0.06 wt % (nanocomposite 1), 0.19 wt % (nanocomposite 2) and 0.35 wt % (nanocomposite 3). Materials were strongly colored as a consequence of the high extinction coefficient of silver NPs but did not show opalescence which indicates absence of scattering due to aggregation phenomena.

UV−visible spectra of the films are shown in Figure 10. The spectrum for the nanocomposite with the highest concentration of

(56) Luedtke, W. D.; Landmann, U. *J. Phys. Chem.* **1996**, *100*, 13323.

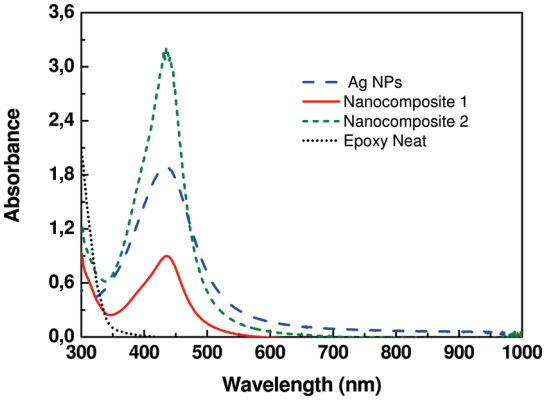

Figure 10. UV−visible absorption spectra for the neat epoxy, a solution of silver NPs and nanocomposites 1 and 2.

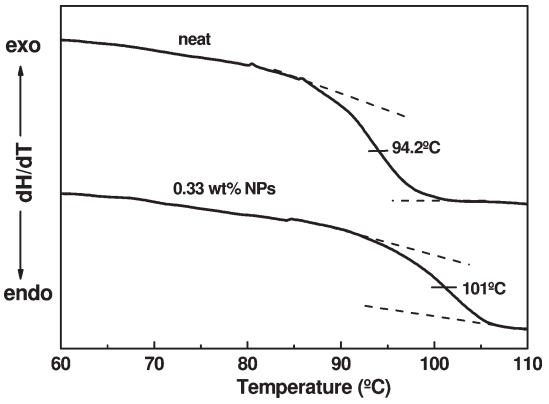

Figure 11. DSC thermograms for the neat epoxy and for the nanocomposite with 0.33 wt % silver NPs.

NPs could not be measured because of saturation of absorbance as a consequence of the high absorption coefficient of NPs. The location of the plasmon band did not exhibit any significant shift in the nanocomposites with respect to the one of the initial dispersion of silver NPs. Moreover, there was no contribution from long wavelength scattering confirming the absence of aggregation phenomena.

The chemical bonding of NPs to the epoxy matrix was confirmed by immersing the samples in THF for 3 months. After this period, no coloration of the solvent was observed. UV−visible spectra of the supernatant did not show the presence of the plasmon band of silver NPs. The conclusion is that NPs are strongly bonded to the epoxy matrix.

The attachment of silver NPs to the epoxy matrix can produce a shift of the glass transition temperature (T_g) due to different effects: (a) chain transfer reactions produce a decrease of the length of primary chains generated in the homopolymerization leading to a decrease of T_g; (b) silver NPs act as macro cross-links of the epoxy network increasing T_g; (c) increasing the concentration of silver NPs can produce nanoconfinement effects in the epoxy network with an expected increase of T_g when polymer chains are covalently bonded to the NPs.[57]

Figure 11 shows DSC thermograms for the neat epoxy and for the nanocomposite with 0.33 wt % silver NPs. The nanocomposite exhibited an increase of about 7 °C in the glass transition temperature with respect to the unmodified epoxy matrix. This

(57) Srivastava, S.; Basu, J. K. *Phys. Rev. Lett.* **2007**, *98*, 165701 and references therein.

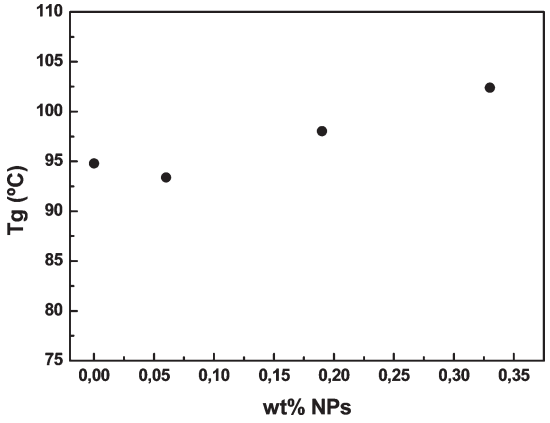

Figure 12. Variation of the glass transition temperature of the nanocomposites with the concentration of silver NPs.

trend was confirmed in duplicate determinations. Figure 12 shows the effect of the concentration of NPs on the T_g of the nanocomposites. The experimental trend may be explained on the basis that chain transfer effects are more important at low concentrations while either one or both of the other two effects (macro cross-links and nanoconfinement) prevail at high concentrations.

Apart from the obvious use of silver NPs to obtain colored epoxy coatings, a number of potential applications may be envisaged for this kind of nanocomposite. For example antibacterial epoxy coatings based on the action of silver NPs might be developed. Although the mechanism of the bactericidal effect of silver NPs is not completely understood, several studies propose that Ag NPs may attach to the surface of the cell membrane or even penetrate inside the bacteria disturbing permeability and respiration functions of the cell.[58] In proteomic and biochemical studies, nanomolar concentrations of Ag NPs have killed *Escherichia coli* cells within minutes possibly due to immediate dissipation of the proton motive force, an action similar to that found for antimicrobial activities of Ag^+ ions.[58] The effective concentration of Ag NPs was at nanomolar levels while Ag^+ ions were effective at micromolar levels. Therefore Ag NPs seem to be more efficient than Ag^+ ions in performing antimicrobial activities. Moreover, silver NPs attached to a polymer matrix also exhibit bactericidal properties.[59]

Using a high concentration of silver NPs could generate coatings with antistatic properties[60] or materials with high dielectric constants that can be used for capacitors or energy storage devices.[61] The structure of the nanoparticles (hard core−soft shell) associated with a very high surface area per unit volume might produce a significant enhancement in the toughness of the epoxy matrix, a similar effect as the one observed when dispersing micelles of block copolymers.[62]

Conclusions

An original procedure for the synthesis of 4 nm, water-dispersible silver NPs was reported, consisting of a reduction step generating silver clusters followed by an annealing step producing silver NPs stabilized by 11-undecanoate anions. Carboxylate anions were chemically bonded to a monoepoxy compound

(58) Sharma, V. K.; Yngard, R. A.; Lin, Y. *Adv. Colloid Interface Sci.* **2009**, *145*, 83.
(59) Jain, P.; Pradeep, T. *Biotechnol. Bioeng.* **2005**, *90*, 59.
(60) Wakabayashi, A.; Sasakawa, Y.; Dobashi, T.; Yamamoto, T. *Langmuir* **2006**, *22*, 9260.
(61) Arbatti, M.; Shan, X.; Cheng, Z. *Adv. Mater.* **2007**, *19*, 1369.
(62) Ruiz-Pérez, L.; Royston, G. J.; Fairclough, J. P. A.; Ryan, A. J. *Polymer* **2008**, *49*, 4475.

(phenyl glycidyl ether in this study) enabling a shift in the solubility of the NPs from water to a variety of organic solvents. A secondary hydroxyl group was introduced in the organic ligands by the same reaction. The presence of these functional groups can be used for the chemical bonding of the synthesized silver NPs to a variety of materials, substrates and interfaces. We illustrated this possibility analyzing the dispersion and chemical bonding of these NPs into an epoxy network. The resulting colored nanocomposites exhibited constancy in the location of the plasmon band implying that silver NPs were homogeneously dispersed in the epoxy matrix. The glass transition temperature experienced an initial decrease followed by an increase with the NPs concentration. This trend was explained on the basis of changes in the polymer network structure and nanoconfinement effects. Interesting applications for these nanocomposites can be envisaged.

Acknowledgment. We acknowledge the financial support of the National Research Council (CONICET, Argentina), the National Agency for the Promotion of Science and Technology (ANPCyT, Argentina), and the University of Mar del Plata. We thank Federico J. Williams, Tenaris-INQUIMAE (Argentina), for XPS measurements.